Critical endpoint in the continuum limit and critical endline at $N_{\mathrm{T}} = 6$ of the finite temperature phase transition of QCD with clover fermions

Yoshifumi Nakamura[*]

RIKEN Center for Computational Science, Kobe, Hyogo 650-0047, Japan
Graduate School of System Informatics, Department of Computational Sciences, Kobe
University, Kobe, Hyogo 657-8501, Japan
E-mail: nakamura@riken.jp

Yoshinobu Kuramashi

Faculty of Pure and Applied Sciences, University of Tsukuba, Tsukuba, Ibaraki 305-8571, Japan
Center for Computational Sciences, University of Tsukuba, Tsukuba, Ibaraki 305-8577, Japan
E-mail: kuramasi@het.ph.tsukuba.ac.jp

Hiroshi Ohno

Center for Computational Sciences, University of Tsukuba, Tsukuba, Ibaraki 305-8577, Japan
E-mail: hohno@ccs.tsukuba.ac.jp

Shinji Takeda

Institute of Physics, Kanazawa University, Kanazawa 920-1192, Japan
E-mail: takeda@hep.s.kanazawa-u.ac.jp

We investigate the critical endpoints of the finite temperature phase transition of QCD at zero chemical potential. We employ the renormalization-group improved Iwasaki gauge action and non-perturbatively O(a)-improved Wilson-clover fermion action. The critical endpoints are determined by using the intersection point of kurtosis, employing the multi-parameter, multi-ensemble reweighting method. We present results for the critical endline at $N_{\mathrm{T}} = 6$ and the continuum extrapolation for the critical endpoint of the SU(3)-flavor symmetric point.

[*]Speaker.

1. Introduction

The nature of the finite temperature phase transition of 2+1 flavor QCD at zero chemical potential depends on quark masses. The order of transition and universality class are summarized in the plane of light quark mass, m_l and strange quark mass, m_s, which is called the Columbia plot [1].

A first order phase transition is expected in the small quark mass region [2]. Many lattice QCD studies have shown that the phase transition is also of first order in the heavy quark mass region while it is crossover in the medium quark mass region. The boundary between the first order and crossover regions is a second order phase transition of Z_2 universality class.

The nature in the lower-left corner of the Columbia plot has not been fully understood yet. The first lattice QCD calculation was done by using standard Wilson fermions at $N_T = 4$ roughly 20 years ago. It reported the critical mass at the critical endpoint (CEP), m_E, for $N_F = 3$ is heavy: the critical quark mass $m_{q,E} = m_{l,E} = m_{s,E} \gtrsim 140$ MeV or, equivalently, the critical pseudo scalar mass $m_{PS,E} = m_{\pi,E} = m_{\eta_s,E} \gtrsim 1$ GeV [3]. After a preliminary study with standard Wilson gauge and staggered fermions which reported the bare critical mass $am_{q,E} \sim 0.035$ [4] at $N_T = 4$, Karsch *et al.* reported preliminary values for the critical mass, $m_{PS,E} \sim 290$ MeV with unimproved gauge and staggered fermion actions and $m_{PS,E} \sim 190$ MeV with improved gauge and p4 staggered fermion actions [5]. These results were obtained by using the R-algorithm [6]. Afterward, the results were updated as $m_{PS,E} = 290(20)$ MeV with unimproved gauge and staggered fermion actions and $m_{PS,E} = 67(17)$ MeV with improved gauge and p4 staggered fermion actions [7]. Then, in ref. [8], de Forcrand and Philipsen obtained $am_{q,E} = 0.0260(5)$ by using the RHMC algorithm [9, 10], which is about 25% smaller than the value $am_{q,E} \approx 0.033$ quoted by works using the R-algorithm. They also performed $N_F = 2 + 1$ simulations and obtained the critical line and tri-critical point, $am_s^{tri} \approx 0.7$, where lattice spacing a was approximately 0.3 fm. In ref. [11] with unimproved staggered fermions, it was reported that the ratio of $m_{PS,E}$ and the CEP temperature T_E decreased from 1.680(4) to 0.954(12) as increasing N_T from 4 to 6. These results are showing very large cut off effect for the critical mass and it is important to increase N_T and use improved actions. Further studies with improved staggered fermions have not found the first order phase transition and quoted only a bound of the critical mass, $m_{PS,E} \lesssim 50$ MeV, [12, 13, 14]. Therefure, the positions of the critical endline (CEL), m_s^{tri} and CEP for $N_F = 3$ are still particularly important problems to be solved at this moment.

Recently we also have investigated the nature of the finite phase transition in the small quark mass region by using non-perturbatively $O(a)$-improved Wilson-clover fermions. We have determined CEP at $N_T = 4, 6, 8$, and 10 as well as an upper bound of CEP in the continuum limit for $N_F = 3$ [15, 16]. For $N_F = 2 + 1$, we have studied at $N_T = 6$ and determined CEL around the SU(3) flavor symmetric point. Then, we confirmed that the slope of CEL at the SU(3) flavor symmetric point is -2 [17]. In this paper, we extend our study for both CEP at the SU(3) flavor symmetric point and CEL away from the SU(3) flavor symmetric point.

2. Simulations

We employ the renormalization-group improved Iwasaki gauge action [18] and non-perturbatively

$O(a)$-improved Wilson-clover fermion action [19]. CEP is determined by using the intersection point of kurtosis of chiral condensate. This method is expounded in Ref [15] and used in our recent studies [15, 16, 17]. Expectation value, susceptibility and skewness of chiral condensate are also used for confirming phase transition and determination of the transition point. Chiral condensate and its higher moments are computed from traces of the inverse Wilson clover Dirac operator up to a power of -4, *i.e.* $\text{Tr}D^{-1,-2,-3,-4}$, by using 10 noise vectors. We have checked that 10 noises are good enough in this study. We employ the multi-parameter, multi-ensemble reweighting method [20] to determine CEP with very small statistical error. We reweight both κ_l and κ_s so that we can determine many CEPs without doing simulations at many parameter sets. We performed zero temperature runs for physical scale setting which are covering almost all transition points of finite temperature simulations. Lattice spacings are computed by the Wilson flow lattice scale $\sqrt{t_0}/a$ [21]. Our finite temperature simulations are performed at the temporal size $N_T = 6$ and with a lattice spacing $a \approx 0.19$ fm for CEL, and $N_T = 12$ and $a \approx 0.12$ fm for the continuum limit of CEP at the SU(3) flavor symmetric point. The spatial size N_S is $10, 12, 16,$ and 24 at $N_T = 6$ and $N_S = 16, 20, 24, 28,$ and 32 at $N_T = 12$. We have confirmed $m_{PS}L > 4$ at almost all transition points, where m_{PS} is the pseudo scalar mass and L is the physical spatial extent. We will explain complete simulation details in our upcoming full paper.

3. Simulation results

3.1 Simulation results for $N_F = 3$

We show expectation value, susceptibility, skewness and kurtosis of chiral condensate at $\beta = 1.80$ as example in Fig. 1. It shows that the reweighting method works well and we can find the phase transition precisely. Fig. 2 shows a kurtosis intersection plot and a plot for the ratio of the critical exponents, $b = \gamma/\nu$ determined by finite size scaling of the peak height of susceptibility, $\chi_{\max} = N_S^b$. To locate the intersection point of kurtosis we use a following modified fitting form including a correction term from energy-like observable that we have used in our previous study:

$$K = \left[K_E + A N_S^{1/\nu}(\beta - \beta_E) \right] \left(1 + B N_S^{y_t - y_h} \right), \tag{3.1}$$

wherer K, K_E, β_E, y_t, and y_h are kurtosis, kurtosis at the endpoint, β at the endpoint, the exponent for the temperature and the magnetic field, respectively. We examine three fits as follows. Fit-1 has no correction term ($B = 0$) and all other parameters are used as fit parameters. Fit-2 also neglects the correction term assuming the 3D Z_2 universality class for K_E and ν. Fit-3 includes the correction term assuming the 3D Z_2 universality class for K_E, ν, and $y_t - y_h$. In the 3D Z_2 universality class, $K_E = -1.396$, $\nu = 0.63$, and $y_t - y_h = -0.894$. The fit results are summarized in Table 1. Fit-1 gives substantially larger K_E than the 3D Z_2 value with large error. ν is consistent with the universal value 0.63 but it has fairly large error. So we can not confirm transition belongs to the 3D Z_2 universality class from Fit-1. We observe $\chi^2/\text{d.o.f.}$ of Fit-2, assuming the 3D Z_2 universality class without correction term, is not bad and reasonable $\chi^2/\text{d.o.f.} < 1$ for Fit-3.

For a cross check of the endpoint location, a b plot (right panel of fig. 2) is helpful because b changes from dimension number (3 in this study) to 0 via a certain value at the critical endpoint when the transition changes from the first order phase transtion to crossover. The value of a green

horizontal line is b of the 3D Z_2 universality class. We see b as a fuction of β is crossing the green line at β_E determined by the kurtosis intersection. This cross check tells our analysis works well. We adopt β_E determined by Fit-3 in the following analysis. Since b of other universality classes is a similar value as b of the 3D Z_2 universality class, this plot is not suited to distinguish the universality class.

In Fig. 3, $m_{PS,E}$ and T_E normalized by $\sqrt{t_0}$ as a function of $1/N_T^2$ are shown. Linear continuum extrapolations give $\sqrt{t_0}m_{PS} = 0.1262(57)$ with $\chi^2/\text{d.o.f.} = 0.84$ and $\sqrt{t_0}T = 0.09968(36)$ with $\chi^2/\text{d.o.f.} = 0.34$
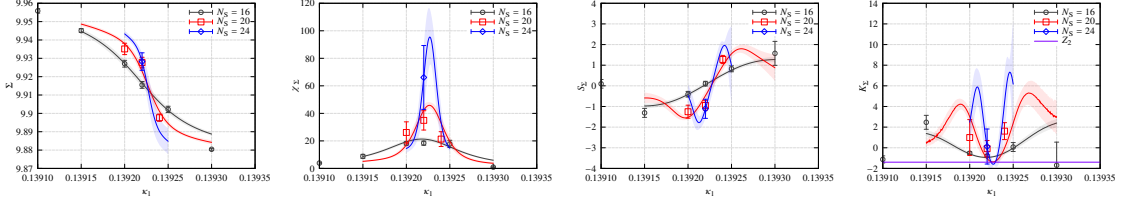

Figure 1: Expectation value , susceptibility, skewness and kurtosis of chiral condensate as a function of κ at $\beta = 1.80$.
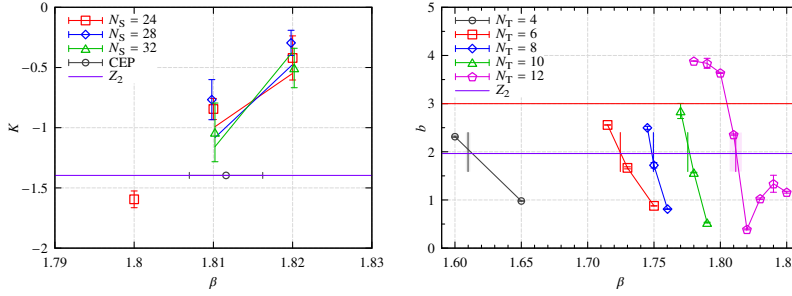

Figure 2: Kurtosis intersection (left) and the ratio of the critical exponents, $b = \gamma/\nu$ (right) as a function of β for $N_F = 3$ including smaller N_T results.

Table 1: Kurtosis intersection fitting reuslts for $N_F = 3$.

Fit	β_E	K_E	ν	A	B	$y_t - y_h$	$\chi^2/\text{d.o.f.}$
1	1.8145(42)	$-0.64(21)$	0.66(56)	0.4(1.5)	0	0	0.34
2	1.7954(66)	-1.396	0.63	0.211(69)	0	0	1.34
3	1.8098(26)	-1.396	0.63	0.419(89)	$-7.0(1.5)$	-0.894	0.29

3.2 Simulation results for $N_F = 2 + 1$

In Fig. 4, we plot CEP in two different bare parameter planes: $(1/\kappa_l, 1/\kappa_s)$-plane and $(\beta, 1/\kappa_s)$-plane. Fig. 5 shows CEP at $N_T = 6$ together with preliminary results for CEL at $N_T = 6, 8$, and 10 as well as its continuum extrapolation in a dimensionless physical scale plane. This plane corresponds a light quark and strange quark mass plane. We see that CEL blows up rapidly as decreasing the light quark mass. We will explain how to estimate CEL at $N_T > 6$ later.
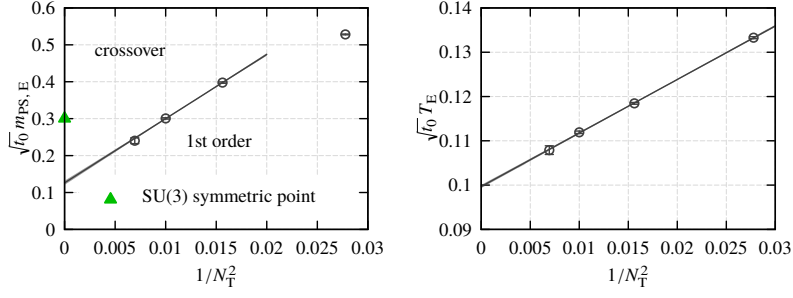
Figure 3: Continuum extrapolations for $\sqrt{t_0}m_{\text{PS,E}}$ (left) and $\sqrt{t_0}T_{\text{E}}$ (right).
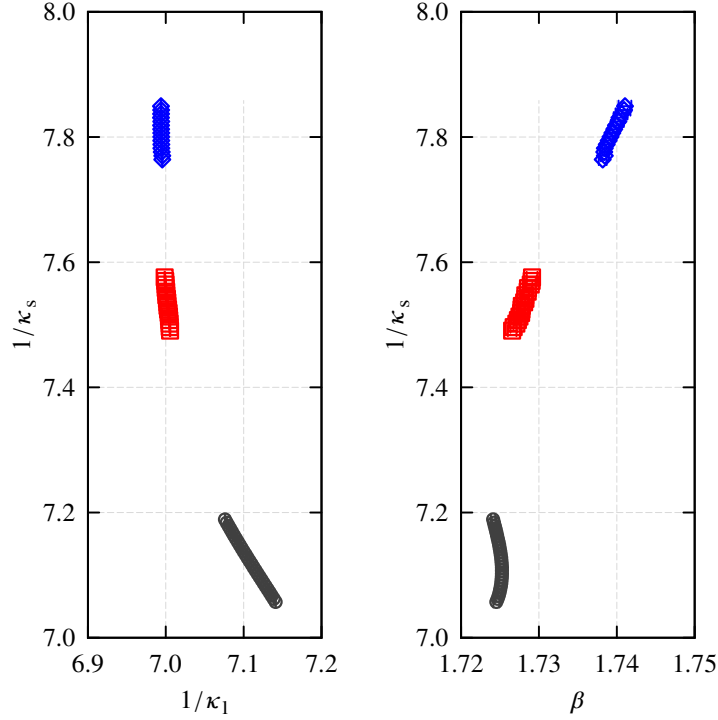

Figure 4: CEP in bare parameter planes.

To estimate CEL, we first fit CEP at $N_{\text{T}} = 6$ to a formula inspired by the tri-critical scaling law [22]

$$y = b_0 + b_1 x^{2/5}, \tag{3.2}$$

where $x = (\sqrt{t_0}m_{\pi,\text{E}})^2$, $y = (\sqrt{t_0}m_{\eta_s,\text{E}})^2$, b_0 and b_1 are free parameters. Resulting b_0 is proportional to the strange quark mass at the tri-critical point. We obtain $b_0 = 6.71(8)$ and $b_1 = -13.3(2)$ with $\chi^2/\text{d.o.f.} = 0.54$ by using only data in range $x < 0.105$, *i.e.* $m_{\eta_s,\text{E}}^2/m_{\pi,\text{E}}^2 > 10$. By changing the fitting range in this fitting, we can discuss the tri-critical scaling region. Since the fitting which includes data up to $x \approx 0.125$ gives reasonable $\chi^2/\text{d.o.f.}$, that is less than one, we update the tentative scaling region at $N_{\text{T}} = 6$, *i.e.* $m_{\eta_s,\text{E}}^2/m_{\pi,\text{E}}^2 > 7.5$.

In the all range fitting we use the formula adding a power series up to terms of order x^5 to
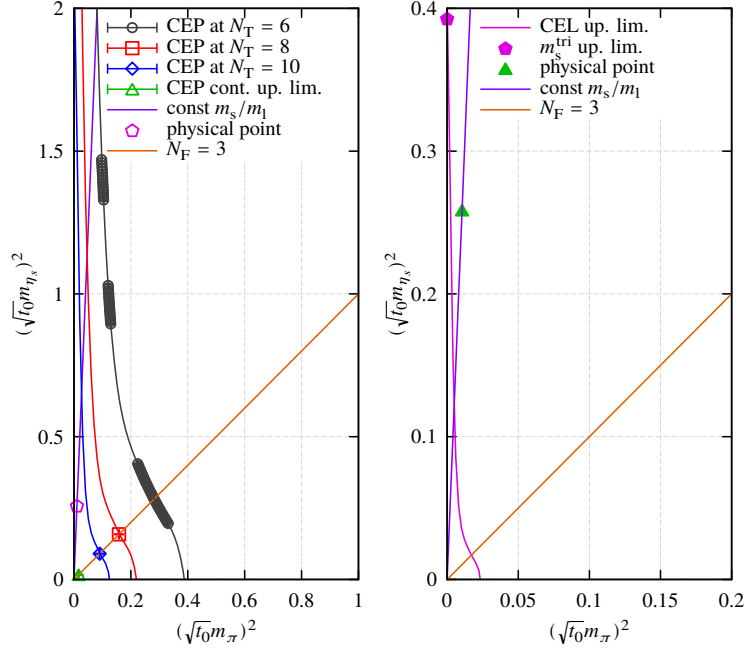
Figure 5: Preliminary results for CEL at $N_T = 6, 8$, and 10 (left), and in the continuum limit (right).

eq. (3.2)

$$y = b_0 + a_0 x^{2/5} + \sum_{i=1}^{5} a_i x^i, \tag{3.3}$$

where $b_0 = 6.71$ and a_i are free parameters. By fixing b_0 we obtain reasonable χ^2/d.o.f., 1.3. We could not find reasonable fitting neither without fixing b_0 nor with less polynomial order fitting functions.

Further estimation is possible by using results for $N_F = 3$ and assuming that there is no N_T dependence in the shape of CEL. The normalized pseudo scalar masses at CEP and the SU(3) flavor symmetric point for each N_T, $\sqrt{t_0} m_{PS,E,N_T}^{sym}$ are

$$\begin{aligned}
\sqrt{t_0} m_{PS,E,6}^{sym} &= 0.5282(12), \quad &\sqrt{t_0} m_{PS,E,8}^{sym} &= 0.3977(19), \\
\sqrt{t_0} m_{PS,E,10}^{sym} &= 0.3006(19), \quad &\sqrt{t_0} m_{PS,E,\infty}^{sym} &< 0.1281(61),
\end{aligned} \tag{3.4}$$

where the result in the continuum limit (at $N_T = \infty$) is an upper bound. Since the updated continuum limit of CEP at the SU(3) flavor symmetric point is still preliminary, we estimate the upper bound of CEL in the continuum limit by using previous published results [16]. For example, we obtain CEL at $N_T = 8$ by scaling $\sqrt{t_0} m_{\pi,E}$ and $\sqrt{t_0} m_{\eta_s,E}$ by the ratio of $\sqrt{t_0} m_{PS,E,8}^{sym}$ to $\sqrt{t_0} m_{PS,E,6}^{sym}$. On the above assumption, we find $m_s^{tri} \lesssim 1.5 m_s^{phy}$ in the continuum limit.

4. Summary

We have determined CEP at the SU(3)-flavor symmetric point at $N_T = 12$, and CEL away from the SU(3)-flavor symmetric point at $N_T = 6$ with non-perturbatively $O(a)$-improved Wilson

fermions. We presented preliminary results for CEP in the continuum limit and CEL at $N_T = 8, 10$ and in the continuum limit. We found that a linear continuum extrapolation including new data is reasonable and gives preliminary results at CEP in the continuum limit: $\sqrt{t_0} m_{PS} = 0.1262(57)$, $\sqrt{t_0} T = 0.09968(36)$. Moreover, 3 series of multi-ensemble, multi-parameter reweighting well determine CEL, where CEL at $N_T = 6$ is nice agreement with $m_s - m_s^{tri} \sim m_l^{2/5}$ in the small m_l region, with $m_s^{tri} \lesssim 1.5 m_s^{phy}$ as a very preliminary result.

References

[1] F.R. Brown, F.P. Butler, H. Chen, N.H. Christ, Z.h. Dong, W. Schaffer, L.I. Unger, A. Vaccarino, Phys. Rev. Lett. **65**, 2491 (1990)

[2] R.D. Pisarski, F. Wilczek, Phys. Rev. **D29**, 338 (1984)

[3] Y. Iwasaki, K. Kanaya, S. Kaya, S. Sakai, T. Yoshie, Phys. Rev. **D54**, 7010 (1996), `hep-lat/9605030`

[4] S. Aoki et al. (JLQCD), Nucl. Phys. Proc. Suppl. **73**, 459 (1999), `hep-lat/9809102`

[5] F. Karsch, E. Laermann, C. Schmidt, Phys. Lett. **B520**, 41 (2001), `hep-lat/0107020`

[6] S.A. Gottlieb, W. Liu, D. Toussaint, R.L. Renken, R.L. Sugar, Phys. Rev. **D35**, 2531 (1987)

[7] F. Karsch, C.R. Allton, S. Ejiri, S.J. Hands, O. Kaczmarek, E. Laermann, C. Schmidt, Nucl. Phys. Proc. Suppl. **129**, 614 (2004), [,614(2003)], `hep-lat/0309116`

[8] P. de Forcrand, O. Philipsen, JHEP **01**, 077 (2007), `hep-lat/0607017`

[9] M.A. Clark, A.D. Kennedy, Z. Sroczynski, Nucl. Phys. Proc. Suppl. **140**, 835 (2005), [,835(2004)], `hep-lat/0409133`

[10] M.A. Clark, A.D. Kennedy, Phys. Rev. Lett. **98**, 051601 (2007), `hep-lat/0608015`

[11] P. de Forcrand, S. Kim, O. Philipsen, PoS **LAT2007**, 178 (2007), `0711.0262`

[12] G. Endrodi, Z. Fodor, S.D. Katz, K.K. Szabo, PoS **LAT2007**, 182 (2007), `0710.0998`

[13] H.T. Ding, A. Bazavov, P. Hegde, F. Karsch, S. Mukherjee, P. Petreczky, PoS **LATTICE2011**, 191 (2011), `1111.0185`

[14] A. Bazavov, H.T. Ding, P. Hegde, F. Karsch, E. Laermann, S. Mukherjee, P. Petreczky, C. Schmidt, Phys. Rev. **D95**, 074505 (2017), `1701.03548`

[15] X.Y. Jin, Y. Kuramashi, Y. Nakamura, S. Takeda, A. Ukawa, Phys. Rev. **D91**, 014508 (2015), `1411.7461`

[16] X.Y. Jin, Y. Kuramashi, Y. Nakamura, S. Takeda, A. Ukawa, Phys. Rev. **D96**, 034523 (2017), `1706.01178`

[17] Y. Kuramashi, Y. Nakamura, S. Takeda, A. Ukawa, Phys. Rev. **D94**, 114507 (2016), `1605.04659`

[18] Y. Iwasaki (1983), `1111.7054`

[19] S. Aoki et al. (JLQCD, CP-PACS), Phys. Rev. **D73**, 034501 (2006), `hep-lat/0508031`

[20] A.M. Ferrenberg, R.H. Swendsen, Phys. Rev. Lett. **61**, 2635 (1988)

[21] M. Lüscher, JHEP **08**, 071 (2010), [Erratum: JHEP03,092(2014)], `1006.4518`

[22] K. Rajagopal (1995), `hep-ph/9504310`